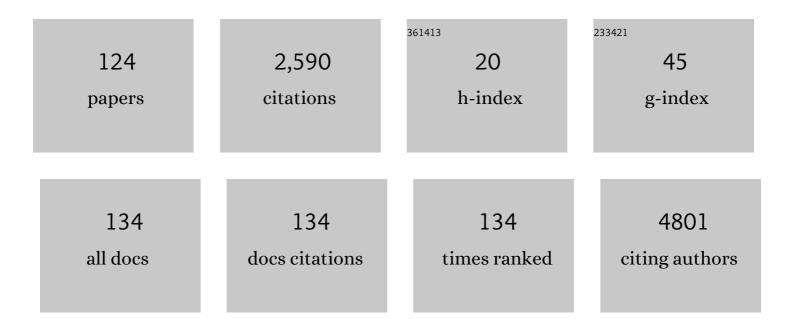
List of Publications by Year in descending order

Source: https://exaly.com/author-pdf/1455106/publications.pdf Version: 2024-02-01



7uenti

#	Article	IF	CITATIONS
1	Clinical characteristics, risk factors and outcomes of cancer patients with <scp>COVID</scp> â€19: A populationâ€based study. Cancer Medicine, 2023, 12, 287-296.	2.8	3
2	Mass Screening for Low Bone Density Using Basic Check-Up Items. IEEE Transactions on Computational Social Systems, 2023, 10, 2579-2586.	4.4	2
3	3-D Textural Analysis of 2-[¹âɟF]FDG PET and Ki67 Expression in Nonsmall Cell Lung Cancer. IEEE Transactions on Radiation and Plasma Medical Sciences, 2022, 6, 113-120.	3.7	1
4	Hemodynamic effect through a novel endoscopic intervention in management of varices and hypersplenism (with video). Gastrointestinal Endoscopy, 2022, 95, 172-183.e2.	1.0	7
5	Evaluation of a fractional-order calculus diffusion model and bi-parametric VI-RADS for staging and grading bladder urothelial carcinoma. European Radiology, 2022, 32, 890-900.	4.5	16
6	Body composition in relation to postoperative anastomotic leakage and overall survival in patients with esophageal cancer. Nutrition, 2022, 94, 111534.	2.4	9
7	Multiparametric <scp>MRI</scp> â€Based Radiomic Signature for Preoperative Evaluation of Overall Survival in Intrahepatic Cholangiocarcinoma After Partial Hepatectomy. Journal of Magnetic Resonance Imaging, 2022, 56, 739-751.	3.4	9
8	Accuracy and Challenges in the Vesical <scp>Imagingâ€Reporting</scp> and Data System for Staging Bladder Cancer. Journal of Magnetic Resonance Imaging, 2022, 56, 391-398.	3.4	7
9	Noninvasive assessment of clinical and pathological characteristics of patients with IgA nephropathy by diffusion kurtosis imaging. Insights Into Imaging, 2022, 13, 18.	3.4	5
10	Novel imaging phenotypes of naÃ ⁻ ve asthma patients with distinctive clinical characteristics and T2 inflammation traits. Therapeutic Advances in Chronic Disease, 2022, 13, 204062232210848.	2.5	1
11	DWI-based radiomic signature: potential role for individualized adjuvant chemotherapy in intrahepatic cholangiocarcinoma after partial hepatectomy. Insights Into Imaging, 2022, 13, 37.	3.4	3
12	Renal functional and interstitial fibrotic assessment with non-Gaussian diffusion kurtosis imaging. Insights Into Imaging, 2022, 13, 70.	3.4	2
13	The Role of the Superior Cervical Sympathetic Ganglion in Ischemia Reperfusion-Induced Acute Kidney Injury in Rats. Frontiers in Medicine, 2022, 9, 792000.	2.6	2
14	Case Report: "Area of Focus―Atypical Trichinellosis and Fascioliasis Coinfection. Frontiers in Medicine, 2022, 9, .	2.6	2
15	Ureteral calculi lithotripsy for single ureteral calculi: can DNN-assisted model help preoperatively predict risk factors for sepsis?. European Radiology, 2022, 32, 8540-8549.	4.5	5
16	Partial splenic embolization through endoscopic ultrasound-guided implantation of coil as a potential technique to treat portal hypertension. Endoscopy, 2021, 53, E40-E41.	1.8	7
17	One-stop assessment of renal function and renal artery in hypertensive patients with suspected renal dysfunction: non-enhanced MRI using spatial labeling with multiple inversion pulses. European Radiology, 2021, 31, 94-103.	4.5	3
18	Evaluation of hepatic steatosis before liver transplantation in ex vivo by volumetric quantitative PDFFâ€MRI. Magnetic Resonance in Medicine, 2021, 85, 2805-2814.	3.0	2

#	Article	IF	CITATIONS
19	Prediction of the World Health Organization Grade of rectal neuroendocrine tumors based on CT histogram analysis. Cancer Medicine, 2021, 10, 595-604.	2.8	9
20	â€~Curved tunnel' sign on MRI: a typical radiological feature in hepatic trichinellosis. Abdominal Radiology, 2021, 46, 2584-2594.	2.1	3
21	Predictive factors of postoperative pancreatic fistula after laparoscopic pancreatoduodenectomy. Annals of Translational Medicine, 2021, 9, 41-41.	1.7	6
22	Bone Fragment Co-transplantation Alongside Bone Marrow Aspirate Infusion Protects Kidney Transplant Recipients. Frontiers in Immunology, 2021, 12, 630710.	4.8	1
23	Primary Gastro-Intestinal Lymphoma and Gastro-Intestinal Adenocarcinoma: An Initial Study of CT Texture Analysis as Quantitative Biomarkers for Differentiation. Life, 2021, 11, 264.	2.4	0
24	Application of bi-planar reduced field-of-view DWI (rFOV DWI) in the assessment of muscle-invasiveness of bladder cancer. European Journal of Radiology, 2021, 136, 109486.	2.6	14
25	Morphometric assessment of the mesorectal fat in Chinese Han population: A clinical MRI study. Science Progress, 2021, 104, 003685042110162.	1.9	3
26	Combining volumetric apparent diffusion coefficient histogram analysis with vesical imaging reporting and data system to predict the muscle invasion of bladder cancer. Abdominal Radiology, 2021, 46, 4301-4310.	2.1	14
27	Comparison of reduced field-of-view diffusion-weighted imaging (DWI) and conventional DWI techniques in the assessment of Cervical carcinoma at 3.0T: Image quality and FIGO staging. European Journal of Radiology, 2021, 137, 109557.	2.6	21
28	CT facilitates improved diagnosis of adult intestinal malrotation: a 7-year retrospective study based on 332 cases. Insights Into Imaging, 2021, 12, 58.	3.4	12
29	Correlation of [18F]florbetaben textural features and age of onset of Alzheimer's disease: a principal components analysis approach. EJNMMI Research, 2021, 11, 40.	2.5	3
30	Hemodynamic study of unenhanced magnetic resonance angiography using spatial labeling with multiple inversion pulses sequence: a phantom study. Quantitative Imaging in Medicine and Surgery, 2021, 11, 1828-1835.	2.0	1
31	Quantitative T2*-Weighted Imaging and Reduced Field-of-View Diffusion-Weighted Imaging of Rectal Cancer: Correlation of R2* and Apparent Diffusion Coefficient With Histopathological Prognostic Factors. Frontiers in Oncology, 2021, 11, 670156.	2.8	8
32	Utility of noncontrast MRI in the detection and risk grading of gastrointestinal stromal tumor: a comparison with contrast-enhanced CT. Quantitative Imaging in Medicine and Surgery, 2021, 11, 2453-2464.	2.0	6
33	Genome-wide association study of COVID-19 severity among the Chinese population. Cell Discovery, 2021, 7, 76.	6.7	41
34	Serum semaphorin4C as an auxiliary diagnostic biomarker for breast cancer. Clinical and Translational Medicine, 2021, 11, e480.	4.0	3
35	A Chinese host genetic study discovered IFNs and causality of laboratory traits on COVID-19 severity. IScience, 2021, 24, 103186.	4.1	10
36	Computed tomography-based multiple body composition parameters predict outcomes in Crohn's disease. Insights Into Imaging, 2021, 12, 135.	3.4	14

#	Article	IF	CITATIONS
37	Comparison and development of preoperative systemic inflammation markers-based models for the prediction of unfavorable pathology in newly diagnosed clinical T1 renal cell carcinoma. Pathology Research and Practice, 2021, 225, 153563.	2.3	4
38	Clinical and Radiological Features of Urachal Carcinoma and Infection. Frontiers in Oncology, 2021, 11, 702116.	2.8	4
39	Metal ions-mediated self-assembly of nanomedicine for combinational therapy against triple-negative breast cancer. Chemical Engineering Journal, 2021, 425, 131420.	12.7	13
40	â€~Curved tunnel' sign on MRI: a typical radiological feature in hepatic trichinellosis. , 2021, 46, 2584.		1
41	Assessment of renal function using magnetic resonance quantitative histogram analysis based on spatial labeling with multiple inversion pulses. Annals of Translational Medicine, 2021, 9, 1614-1614.	1.7	2
42	Noninvasive assessment of kidney dysfunction in children by using blood oxygenation level-dependent MRI and intravoxel incoherent motion diffusion-weighted imaging. Insights Into Imaging, 2021, 12, 146.	3.4	12
43	L-EGCC-Mn nanoparticles as a pH-sensitive MRI contrast agent. Drug Delivery, 2021, 28, 126-135.	5.7	4
44	The Preventive Effect of Cardiac Sympathetic Denervation Induced by 6-OHDA on Myocardial Ischemia–Reperfusion Injury: The Changes of IncRNA/circRNAs-miRNA-mRNA Network of the Upper Thoracic Spinal Cord in Rats. Oxidative Medicine and Cellular Longevity, 2021, 2021, 1-28.	4.0	7
45	Advancing COVID-19 diagnosis with privacy-preserving collaboration in artificial intelligence. Nature Machine Intelligence, 2021, 3, 1081-1089.	16.0	30
46	A magnetic resonance nanoprobe with STING activation character collaborates with platinum-based drug for enhanced tumor immunochemotherapy. Journal of Nanobiotechnology, 2021, 19, 415.	9.1	3
47	Magnetic resonance imaging-based body composition is associated with nutritional and inflammatory status: a longitudinal study in patients with Crohn's disease. Insights Into Imaging, 2021, 12, 178.	3.4	5
48	The connectome from the cerebral cortex to the viscera using viral transneuronal tracers American Journal of Translational Research (discontinued), 2021, 13, 12152-12167.	0.0	0
49	Assessment of renal fibrosis in a rat model of unilateral ureteral obstruction with diffusion kurtosis imaging: Comparison with α-SMA expression and 18F-FDG PET. Magnetic Resonance Imaging, 2020, 66, 176-184.	1.8	10
50	Evaluation of a Digital Brain Positron Emission Tomography Scanner Based on the Plug&Imaging Sensor Technology. IEEE Transactions on Radiation and Plasma Medical Sciences, 2020, 4, 327-334.	3.7	16
51	Application of R2* and Apparent Diffusion Coefficient in Estimating Tumor Grade and T Category of Bladder Cancer. American Journal of Roentgenology, 2020, 214, 383-389.	2.2	16
52	Visceral Adiposity and High Intramuscular Fat Deposition Independently Predict Critical Illness in Patients with SARSâ€CoVâ€2. Obesity, 2020, 28, 2040-2048.	3.0	89
53	Gallbladder carcinoma: an initial clinical experience of reduced field-of-view diffusion-weighted MRI. Cancer Imaging, 2020, 20, 50.	2.8	11
54	Risk of nodal disease in patients with MRI-detected extramural vascular invasion in rectal cancer: a systematic review and meta-analysis. Tumori, 2020, 107, 030089162097586.	1.1	1

#	Article	IF	CITATIONS
55	Clinical Features and Temporal Changes of RT-PCR and Chest CT in COVID-19 Pediatric Patients. Frontiers in Pediatrics, 2020, 8, 579512.	1.9	11
56	Exploration of plasma interleukin-27 levels in asthma patients and the correlation with lung function. Respiratory Medicine, 2020, 175, 106208.	2.9	5
57	A Novel Clinical-Radiomics Model Pre-operatively Predicted the Stone-Free Rate of Flexible Ureteroscopy Strategy in Kidney Stone Patients. Frontiers in Medicine, 2020, 7, 576925.	2.6	18
58	Reduced Field-of-View Diffusion-Weighted Imaging in Histological Characterization of Rectal Cancer: Impact of Different Region-of-Interest Positioning Protocols on Apparent Diffusion Coefficient Measurements. European Journal of Radiology, 2020, 127, 109028.	2.6	7
59	Estimation of Renal Function Using Unenhanced Computed Tomography in Upper Urinary Tract Stones Patients. Frontiers in Medicine, 2020, 7, 309.	2.6	4
60	NEMA-2008 and In-Vivo Animal and Plant Imaging Performance of the Large FOV Preclinical Digital PET/CT System Discoverist 180. IEEE Transactions on Radiation and Plasma Medical Sciences, 2020, 4, 622-629.	3.7	15
61	Manganese threonine chelate—a new enteric contrast agent for MRI: a pilot study on rats. NMR in Biomedicine, 2020, 33, e4293.	2.8	0
62	Clinical and CT features in pediatric patients with COVIDâ€19 infection: Different points from adults. Pediatric Pulmonology, 2020, 55, 1169-1174.	2.0	791
63	Elevated serum levels of S100A8/A9 and HMGB1 at hospital admission are correlated with inferior clinical outcomes in COVID-19 patients. Cellular and Molecular Immunology, 2020, 17, 992-994.	10.5	202
64	Histological grades of rectal cancer: whole-volume histogram analysis of apparent diffusion coefficient based on reduced field-of-view diffusion-weighted imaging. Quantitative Imaging in Medicine and Surgery, 2020, 10, 243-256.	2.0	20
65	Role of Chemical Exchange Saturation Transfer and Magnetization Transfer MRI in Detecting Metabolic and Structural Changes of Renal Fibrosis in an Animal Model at 3T. Korean Journal of Radiology, 2020, 21, 588.	3.4	9
66	Whole-Tumor Quantitative Apparent Diffusion Coefficient Histogram and Texture Analysis to Differentiation of Minimal Fat Angiomyolipoma from Clear Cell Renal Cell Carcinoma. Academic Radiology, 2019, 26, 632-639.	2.5	24
67	Comparison of the Diagnostic Value of Monoexponential, Biexponential, and Stretched Exponential Diffusion-weighted MRI in Differentiating Tumor Stage and Histological Grade of Bladder Cancer. Academic Radiology, 2019, 26, 239-246.	2.5	23
68	Potential of diffusion‑weighted imaging in magnetic resonance enterography to identify neoplasms in the ileocecal region: Use of ultra‑high b‑value diffusion‑weighted imaging. Oncology Letters, 2019, 18, 1451-1457.	1.8	2
69	A Systematic Review of Technical Parameters for MR of the Small Bowel in non-IBD Conditions over the Last Ten Years. Scientific Reports, 2019, 9, 14100.	3.3	7
70	Assessment of tumor heterogeneity: Differentiation of periampullary neoplasms based on CT whole-lesion histogram analysis. European Journal of Radiology, 2019, 115, 1-9.	2.6	24
71	Semi-quantitative visual assessment of hepatic tumor burden can reliably predict survival in neuroendocrine liver metastases treated with transarterial chemoembolization. European Radiology, 2019, 29, 5804-5812.	4.5	13
72	Prognostic value of baseline volumetric multiparametric MR imaging in neuroendocrine liver metastases treated with transarterial chemoembolization. European Radiology, 2019, 29, 5160-5171.	4.5	13

#	Article	IF	CITATIONS
73	Rectal Cancer Invasiveness: Whole-Lesion Diffusion-Weighted Imaging (DWI) Histogram Analysis by Comparison of Reduced Field-of-View and Conventional DWI Techniques. Scientific Reports, 2019, 9, 18760.	3.3	9
74	Hepatoid adenocarcinoma in the peritoneal cavity. Medicine (United States), 2019, 98, e14226.	1.0	4
75	Volumetric Apparent Diffusion Coefficient Histogram Analysis in Differentiating Intrahepatic Massâ€Forming Cholangiocarcinoma From Hepatocellular Carcinoma. Journal of Magnetic Resonance Imaging, 2019, 49, 975-983.	3.4	21
76	Whole-tumor histogram analysis of non-Gaussian distribution DWI parameters to differentiation of pancreatic neuroendocrine tumors from pancreatic ductal adenocarcinomas. Magnetic Resonance Imaging, 2019, 55, 52-59.	1.8	14
77	Quantitative diffusion-weighted magnetic resonance enterography in ileal Crohn's disease: A systematic analysis of intra and interobserver reproducibility. World Journal of Gastroenterology, 2019, 25, 3619-3633.	3.3	5
78	Apparent diffusion coefficient-based histogram analysis differentiates histological subtypes of periampullary adenocarcinoma. World Journal of Gastroenterology, 2019, 25, 6116-6128.	3.3	7
79	Use of the XRCC2 promoter for in vivo cancer diagnosis and therapy. Cell Death and Disease, 2018, 9, 420.	6.3	11
80	Star-shaped polymer of β‑cyclodextrin-g-vitamin E TPGS for doxorubicin delivery and multidrug resistance inhibition. Colloids and Surfaces B: Biointerfaces, 2018, 169, 10-19.	5.0	20
81	The combination of a reduction in contrast agent dose with low tube voltage and an adaptive statistical iterative reconstruction algorithm in CT enterography. Medicine (United States), 2018, 97, e0151.	1.0	11
82	Comparison of reduced fieldâ€ofâ€view diffusionâ€weighted imaging (DWI) and conventional DWI techniques in the assessment of rectal carcinoma at 3.0T: Image quality and histological T staging. Journal of Magnetic Resonance Imaging, 2018, 47, 967-975.	3.4	54
83	Tumor heterogeneity in gastrointestinal stromal tumors of the small bowel: volumetric CT texture analysis as a potential biomarker for risk stratification. Cancer Imaging, 2018, 18, 46.	2.8	35
84	Successful management of multiple-systemic Langerhans cell histiocytosis involving endocrine organs in an adult. Medicine (United States), 2018, 97, e11215.	1.0	8
85	Differentiation of atypical pancreatic neuroendocrine tumors from pancreatic ductal adenocarcinomas: Using wholeâ€ŧumor CT texture analysis as quantitative biomarkers. Cancer Medicine, 2018, 7, 4924-4931.	2.8	50
86	Assessment of different mathematical models for diffusionâ€weighted imaging as quantitative biomarkers for differentiating benign from malignant solid hepatic lesions. Cancer Medicine, 2018, 7, 3501-3509.	2.8	14
87	Subtype Differentiation of Small (≤ cm) Solid Renal Mass Using Volumetric Histogram Analysis of DWI at 3-T MRI. American Journal of Roentgenology, 2018, 211, 614-623.	2.2	36
88	Single extracorporeal shock-wave lithotripsy for proximal ureter stones: Can CT texture analysis technique help predict the therapeutic effect?. European Journal of Radiology, 2018, 107, 84-89.	2.6	16
89	Hepatic Tumors: Diagnosis and Therapeutic Effect Evaluation of Diffusion- Weighted Imaging. Current Medical Imaging, 2018, 14, 172-178.	0.8	2
90	Proton-density fat fraction measurement: A viable quantitative biomarker for differentiating adrenal adenomas from nonadenomas. European Journal of Radiology, 2017, 86, 112-118.	2.6	8

#	Article	IF	CITATIONS
91	Detection of unsuspected pelvic DVTs on abdominopelvic CT scans: a potentially life-saving diagnosis. Emergency Radiology, 2017, 24, 127-131.	1.8	1
92	Differentiating malignant from benign gastric mucosal lesions with quantitative analysis in dual energy spectral computed tomography. Medicine (United States), 2017, 96, e5878.	1.0	14
93	Use of pulmonary CT angiography with low tube voltage and low-iodine-concentration contrast agent to diagnose pulmonary embolism. Scientific Reports, 2017, 7, 12741.	3.3	8
94	Monoexponential, biexponential, and stretched exponential diffusion-weighted imaging models: Quantitative biomarkers for differentiating renal clear cell carcinoma and minimal fat angiomyolipoma. Journal of Magnetic Resonance Imaging, 2017, 46, 240-247.	3.4	39
95	Activation of the Extracellular Signal-Regulated Kinase in the Amygdale Modulates Fentanyl-Induced Hypersensitivity in Rats. Journal of Pain, 2017, 18, 188-199.	1.4	10
96	CaMKIIα may modulate fentanyl-induced hyperalgesia via a CeLC-PAG-RVM-spinal cord descending facilitative pain pathway in rats. PLoS ONE, 2017, 12, e0177412.	2.5	12
97	Developmental anomalies of the right hepatic lobe: systematic comparative analysis of radiological features. Open Life Sciences, 2017, 12, 489-500.	1.4	1
98	Assessing the Early Response of Advanced Cervical Cancer to Neoadjuvant Chemotherapy Using Intravoxel Incoherent Motion Diffusion-weighted Magnetic Resonance Imaging. Chinese Medical Journal, 2016, 129, 665-671.	2.3	22
99	Did low tube voltage CT combined with low contrast media burden protocols accomplish the goal of "double low―for patients? An overview of applications in vessels and abdominal parenchymal organs over the past 5Âyears. International Journal of Clinical Practice, 2016, 70, B5-B15.	1.7	16
100	Adrenal and nephrogenic hypertension: an image quality study of low tube voltage, low-concentration contrast media combined with adaptive statistical iterative reconstruction. International Journal of Clinical Practice, 2016, 70, B29-B36.	1.7	6
101	Inhibition of CaMKIIÂ in the Central Nucleus of Amygdala Attenuates Fentanyl-Induced Hyperalgesia in Rats. Journal of Pharmacology and Experimental Therapeutics, 2016, 359, 82-89.	2.5	17
102	Nonmuscle-invasive and Muscle-invasive Urinary Bladder Cancer. Medicine (United States), 2016, 95, e2951.	1.0	13
103	Small colorectal cancer liver metastases: Clinical value of quantitative iodine-based material decomposition images of spectral CT. World Chinese Journal of Digestology, 2016, 24, 2421.	0.1	0
104	Depiction of Transplant Renal Vascular Anatomy and Complications: Unenhanced MR Angiography by Using Spatial Labeling with Multiple Inversion Pulses. Radiology, 2014, 271, 879-887.	7.3	24
105	Neuroendocrine Liver Metastasis Treated by Using Intraarterial Therapy: Volumetric Functional Imaging Biomarkers of Early Tumor Response and Survival. Radiology, 2013, 266, 502-513.	7.3	54
106	Unresectable Hepatocellular Carcinoma: MR Imaging after Intraarterial Therapy. Part II. Response Stratification Using Volumetric Functional Criteria after Intraarterial Therapy. Radiology, 2013, 268, 431-439.	7.3	49
107	Unresectable Hepatocellular Carcinoma: MR Imaging after Intraarterial Therapy. Part I. Identification and Validation of Volumetric Functional Response Criteria. Radiology, 2013, 268, 420-430.	7.3	41

108 A method for quickly and exactly extracting hepatic vein. , 2013, , .

#	Article	IF	CITATIONS
109	Bilateral uterine artery chemoembolization combined with dilation and curettage for treatment of cesarean scar pregnancy: A method for preserving the uterus. Journal of Obstetrics and Gynaecology Research, 2013, 39, 1153-1158.	1.3	30
110	Islet Cell Liver Metastases: Assessment of Volumetric Early Response with Functional MR Imaging after Transarterial Chemoembolization. Radiology, 2012, 264, 97-109.	7.3	40
111	Intrahepatic Cholangiocarcinoma Treated with Local-Regional Therapy: Quantitative Volumetric Apparent Diffusion Coefficient Maps for Assessment of Tumor Response. Radiology, 2012, 264, 285-294.	7.3	60
112	Diffusion-Weighted Imaging in Abdominal Oncology. Current Medical Imaging, 2012, 8, 82-91.	0.8	1
113	Implementation of an interactive liver surgery planning system. Proceedings of SPIE, 2011, , .	0.8	1
114	Time-dependent changes in CT of radiation-induced liver injury: A preliminary study in gastric cancer patients. Journal of Huazhong University of Science and Technology [Medical Sciences], 2010, 30, 683-686.	1.0	7
115	Bis(4-methylimidazolium) succinate succinic acid solvate. Acta Crystallographica Section E: Structure Reports Online, 2009, 65, o607-o608.	0.2	2
116	Classification of Hepatic Tissues from CT Images Based on Texture Features and Multiclass Support Vector Machines. Lecture Notes in Computer Science, 2009, , 374-381.	1.3	10
117	Enhancement of therapeutic effectiveness by combining liposomal honokiol with cisplatin in ovarian carcinoma. International Journal of Gynecological Cancer, 2008, 18, 652-659.	2.5	46
118	4,4′-Methylenedianilinium bis(3-carboxy-4-hydroxybenzenesulfonate) monohydrate. Acta Crystallographica Section E: Structure Reports Online, 2008, 64, o1947-o1948.	0.2	1
119	Assessment of Gastric Cancer: Value of Two-phase Multidetector-row Spiral CT Three-dimensional Reconstruction Technique. Chinese-German Journal of Clinical Oncology, 2005, 4, 365-368.	0.1	0
120	Effects of Gingko biloba Extract on Gap Junction Changes Induced by Reperfusion/Reoxygenation After Ischemia/Hypoxia in Rat Brain. The American Journal of Chinese Medicine, 2005, 33, 923-934.	3.8	18
121	Diagnostic value of 16 slices spiral-CT for portal vein disorders. Journal of Huazhong University of Science and Technology [Medical Sciences], 2004, 24, 300-302.	1.0	0
122	Cell apoptosis and regeneration of hepatocellular carcinoma after transarterial chemoembolization. World Journal of Gastroenterology, 2004, 10, 1876.	3.3	22
123	Relationship between encephalopathy and portal vein-vena cava shunt: Value of computed tomography during arterial portography. World Journal of Gastroenterology, 2004, 10, 1939.	3.3	4
124	Response to the letter to the editor from Dupouy-Camet et al Abdominal Radiology, 0, , .	2.1	0